Optimized free surface of liquid ^{4}He in hypernetted-chain approximation

M. Saarela, P. Pietiläinen, and A. Kallio
University of Oulu, Department of Theoretical Physics, Linnanmaa SF-90570 Oulu 57, Finland
(Received 12 April 1982)

Within the hypernetted-chain approximation, coupled Euler equations are derived for the radial distribution function and the surface profile of liquid ^{4}He at zero temperature and fixed chemical potential. For the solution a reliable method based on the local-density approximation is developed. It is found that the Euler equation for ρ has a solution only in the region where the bulk pressure is positive and the chemical potential negative. At the saturation point ($\rho_{\rm sat}=0.0175$ Å^{-3} and $E_{\rm sat}/N=-5.2$ K) of our model consisting of the Lennard-Jones potential with de Boer–Michels parameters, we obtain the surface energy $E_s=0.17$ K/Å^2 and the monotonically decreasing surface profile with diffusivity of 6 Å based on (10–90 %) criteria.

I. INTRODUCTION

During recent years the Jastrow method has been very successful in describing the ground-state properties of uniform quantum systems.[1–10] The wave function in this method is constructed from the Jastrow ansatz. With the use of the hypernetted-chain (HNC) approximation, one can relate the Jastrow correlation factor f_{12} to the radial distribution function g_{12} and hence write the total energy $E(g_{12})$ as a functional of g_{12}. The variation of the total energy results in an Euler equation that can be solved for optimized g_{12}.

The success of the above method has encouraged us to go over to nonuniform systems where the number density is a varying function.[11,12] In this work we want to study the planar surface of liquid ^{4}He. the translational invariance of the uniform ^{4}He is broken by introducing an external one-particle pressure field that localizes the density profile. Similar ideas have been employed in the evaluation of the classical liquid-gas and liquid-solid interfaces.[13]

Experimentally, the surface energy of ^{4}He is obtained by extrapolation from finite-temperature measurements giving $E_s=0.274$ K/Å.[14] An indirect estimate of the surface thickness is available from elastic reflectivity for a ^{4}He atom striking the free surface.[15] It was found possible to fit the measured data only when a diffuse surface of 5 Å was adopted.[16]

The surface-density profile is a basic quantity which should be known more accurately than the above numbers indicate in a variety of physical problems. (For review we refer to Refs. 17 and 18.) The binding energies of single H, D, and T atoms to the free surface of liquid ^{4}He,[19] the properties of the ^{3}He layer on top of the ^{4}He surface, ripplon spectrum, etc., all assume the density profile to be known quite accurately.

Theoretical calculations of the ^{4}He-density profile can be divided into two categories—the density functional and the variational. The first approach is exact in principle,[20] but in practice one invokes the concept of local uniformity to obtain approximate forms for the free energy $F(\rho)$ as a functional of the number density ρ. The optimum profile is then determined by the condition $\delta F(\rho)/\delta\rho=0$.[21] It was argued by Ebner and Saam[22] that this procedure leaves out important contributions arising from the zero-point motion of the surface due to ripplons and phonons reflected at the surface. Subsequently, they present a prescription for renormalizing of the density-functional theory and obtain results that are consistent with the surface-tension measurements.

The variational approach has been applied by Chang and Cohen[23] and by Shih and Woo.[24] Both of them constructed a trial Jastrow-type wave function

$$\psi[\vec{r}_1,\ldots,\vec{r}_N]=\prod_{i=1}^{N}\varphi(\vec{r}_i)\psi_0(\vec{r}_1,\ldots,\vec{r}_N)\,, \quad (1)$$

where

$$\psi_0=\prod_{i,j}f(\vec{r}_i,\vec{r}_j) \quad (2)$$

and $\varphi(\vec{r}_i)$ is the single-particle correlation factor which can be related to the one-particle density through the lowest-order Bogoliubov-Born-Green-Kirkwood-Yvon (BBGKY) equation. In these calculations ψ_0 was chosen to be the ground-state wave

function of a *uniform* system and the radial distribution function was evaluated in the local-density approximation using the second BBGKY equation[24] or HNC and Percus-Yevick (PY) equations.[23] The density profile was expressed in parametric form, and the parameters were determined by minimizing the surface energy. The minimum, however, turns out to be quite shallow, and thus the shape of the profile is not precisely determined.[25]

Liu *et al.*[26] criticized the lack of internal consistency in the above calculations. With Monte Carlo technique they evaluated the one-particle density directly from the definition

$$\rho(\vec{r}_1)=N\frac{\int |\psi|^2 d^3r_2\cdots d^3r_N}{\int |\psi|^2 d^3r_1\cdots d^3r_N} \tag{3}$$

starting from φ and ψ_0 used in Refs. 23 and 24. A marked difference to the earlier profiles was found. The output profiles showed a pronounced surface peak that did not appear in the input profiles. Whether exact Monte Carlo calculations retain the same oscillatory structure is not yet known. Ebner and Saam[22] showed that near the liquid-solid interface, oscillations do exist but they cannot be sustained at the free surface of liquid ^{4}He. This conclusion agrees with our results also.

In this work we express the total energy of ^{4}He as a functional of both one-particle density ρ and radial distribution function g_{12} starting from the Jastrow ansatz of Eq. (1), but allowing the nonuniformity to deform also the Jastrow correlation factor f_{12}. Thus we have *two independent functions* which will be determined through variational procedure. In Sec. II. we develop Euler equations of ρ and g_{12} in general for a Bose fluid in external field. As a special case the uniform Bose fluid comes out naturally when $\rho(\vec{r})\equiv\rho_0$. The equation for g_{12} in this limit agrees with the one defined in Refs. 3, and 4, and the equation for ρ determines the pressure of the bulk fluid.

Because of the computational difficulties it is not possible to solve the set of Euler equations exactly even in the simple geometry of a planar surface. Thus we introduce an approximation scheme where the equation for ρ is treated exactly but the coupling to the two-particle functions g_{12} and f_{12} and the nodal sum N_{12} comes through the local-density approximation. The two-particle functions are evaluated in Sec. III. from the second Euler equation at different values of the density parameter $\bar{\rho}$. Thus we optimize these functions at each local density. In Sec. IV we solve the Euler equation for ρ, and in Sec. V we present results discussing various aspects of our approximation scheme.

II. EULER EQUATIONS

Consider a Bose fluid subject to an external field at absolute zero temperature and fixed chemical potential μ. The free energy of such a system is

$$F=E+PV=\mu N+E_sA\ , \tag{4}$$

where E_s is the surface energy per surface area A, and the internal energy

$$E=\frac{\langle\psi|H|\psi\rangle}{\langle\psi|\psi\rangle}\ . \tag{5}$$

The Hamiltonian for a N-particle system can be written as

$$H=-\frac{\hbar^2}{2m}\sum_{i=1}^{N}\nabla_i^2+\frac{1}{2}\sum_{i\neq j}^{N}V_{12}(|\vec{r}_i-\vec{r}_j|)+\sum_{i=1}^{N}U_{\rm ext}(\vec{r}_i)\ . \tag{6}$$

The interaction V_{12} depends only on the relative distance of two particles and $U_{\rm ext}$ is the single-particle potential.

For the wave function of this system we choose the Jastrow ansatz of Eq. (1) and adopt the definitions for the one-particle density given in Eq. (3) and for the two-particle density written in the usual way:

$$\rho^{(2)}(\vec{r}_1,\vec{r}_2)=N(N-1)\frac{\int |\psi|^2 d^3r_3\cdots d^3r_N}{\int |\psi|^2 d^3r_1\cdots d^3r_N}$$
$$\equiv\rho(\vec{r}_1)\rho(\vec{r}_2)g(\vec{r}_1,\vec{r}_2)\ . \tag{7}$$

The last equation defines the radial distribution function $g_{12}\equiv g(\vec{r}_1,\vec{r}_2)$.

This procedure introduces four unknown quantities: the one- and two-particle correlation factors, the one-particle density, and the radial distribution function. They can be related to each other through the lowest-order BBGKY equation,[11]

$$\frac{\vec{\nabla}_1\rho_1}{\rho_1}=\vec{\nabla}_1\ln\varphi_1+\int d^3r_2\rho_2 g_{12}\vec{\nabla}_1\ln f_{12}^2\ , \tag{8}$$

and the HNC/E equation

$$g_{12}=f_{12}^2e^{N_{12}+E_{12}}\ . \tag{9}$$

Even though the sum of elementary diagrams E_{12} is

shown to improve the saturation properties of the uniform ^{4}He fluid,[4] we shall for simplicity ignore them in this work. The nodal sum N_{12} can be evaluated from the generalized Ornstein-Zernike integral equation[27]

$$N_{12}=\int d^3r_3\rho_3(g_{13}-1)(g_{32}-1-N_{32})\ . \tag{10}$$

Inserting the Jastrow wave function into the energy expression (5) and utilizing Eqs. (8)–(10) we can write out the internal energy as

$$E=\int d^3r_1\left[\frac{\hbar^2}{2m}(\vec{\nabla}_1\sqrt{\rho_1})^2+U_{\rm ext}\rho_1\right]+\frac{1}{2}\int\int d^3r_1d^3r_2\rho_1\rho_2\left[V_{12}g_{12}+\frac{\hbar^2}{m}(\vec{\nabla}_1\sqrt{g_{12}})^2-\frac{\hbar^2}{4m}\vec{\nabla}_1g_{12}\cdot\vec{\nabla}_1N_{12}\right] \tag{11}$$

The kinetic energy part here is evaluated from the Jackson-Feenberg identity.[28]

Our aim is to find a minimum for the surface energy

$$E_s=\frac{E}{A}+\frac{PV}{A}-\mu\frac{N}{A} \tag{12}$$

when the bulk quantities pressure P, chemical potential μ, volume V, surface area A, and number of particles N are kept fixed. The two functions that naturally emerge as independent functions in the variation are the square roots $\sqrt{\rho_1}$ and $\sqrt{g_{12}}$. The Euler equations are then

$$\frac{\delta E_s}{\delta\sqrt{\rho_1}}=-\frac{\hbar^2}{m}\vec{\nabla}_1^2\sqrt{\rho_1}+2\sqrt{\rho_1}\left[U_{\rm ext}-\mu+\frac{1}{2}\int d^3r_2\rho_2(H_{12}+H_{21})-\frac{\hbar^2}{8m}\int d^3r_2d^3r_3\rho_2\rho_3\vec{\nabla}_2g_{23}\cdot\vec{\nabla}_2\frac{\delta N_{23}}{\delta\rho_1}\right]=0 \tag{13}$$

and

$$\frac{\delta E_s}{\delta\sqrt{g_{12}}}=\rho_2\left[-\frac{\hbar^2}{m}\vec{\nabla}_1\cdot(\rho_1\vec{\nabla}_1\sqrt{g_{12}})+\sqrt{g_{12}}\left[\rho_1V_{12}+\frac{\hbar^2}{4m}\vec{\nabla}_1\cdot(\rho_1\vec{\nabla}_1N_{12})\right]\right]-\frac{\hbar}{4m}\sqrt{g_{12}}\int d^3r_3d^3r_4\rho_3\rho_4\vec{\nabla}_3g_{34}\cdot\vec{\nabla}_3\frac{\delta N_{34}}{\delta g_{12}}=0\ . \tag{14}$$

In Eq. (13) we have defined

$$H_{12}\equiv V_{12}g_{12}+\frac{\hbar^2}{m}\left[\vec{\nabla}_1\sqrt{g_{12}})^2-\frac{1}{4}\vec{\nabla}_1g_{12}\cdot\vec{\nabla}_1N_{12}\right]\ . \tag{15}$$

The functional derivatives $\delta N_{23}/\delta\rho_1$ and $\delta N_{34}/\delta g_{12}$ are obtained from the Ornstein-Zernike relation (10). Thus

$$\frac{\delta N_{23}}{\delta\rho_1}=C_{12}C_{13} \tag{16}$$

and

$$\frac{\delta N_{34}}{\delta g_{12}}=\rho_2C_{34}\delta(\vec{r}_1-\vec{r}_3)+\rho_1C_{13}\delta(\vec{r}_2-\vec{r}_4)-\rho_1\rho_2C_{13}C_{24}\ . \tag{17}$$

Here we have introduced the direct correlation function C_{12},

$$C_{12}\equiv g_{12}-1-N_{12}\ , \tag{18}$$

and used the Dirac δ function. The integrals in Eqs. (13) and (14) where the functional derivatives appear are simplified by applying the Ornstein-Zernike relation once more.

We are now ready to write out the two coupled Euler equations for a nonuniform Bose fluid:

$$-\frac{\hbar^2}{2m}\vec{\nabla}_1^2\sqrt{\rho_1}+\sqrt{\rho_1}[W_\rho(1)+U_{\rm ext}(1)]=\mu\sqrt{\rho_1}\ , \tag{19}$$

$$-\frac{\hbar^2}{m\rho_1}\vec{\nabla}_1\cdot(\rho_1\vec{\nabla}_1\sqrt{g_{12}})+\sqrt{g_{12}}[V_{12}+W_g(1,2)]=0\ , \tag{20}$$

where the induced potentials are

$$W_\rho(1)=\tfrac{1}{2}\int d^3r_2\rho_2\left[H_{12}+H_{21}-\frac{\hbar^2}{4m}\vec{\nabla}_2N_{12}\cdot\vec{\nabla}_2C_{12}\right] \tag{21}$$

and

$$W_g(1,2)=\frac{\hbar^2}{2m\rho_1}\left[\vec{\nabla}_1\cdot(\rho_1\vec{\nabla}_1N_{12})-\tfrac{1}{2}\rho_1\int d^3r^3\rho_3\vec{\nabla}_3C_{13}\cdot\vec{\nabla}_3C_{32}\right] . \tag{22}$$

It is instructive to study these equations in the limit of a uniform fluid where the density is constant $\rho(\vec{r})=\rho_0$ and no external potential appears. The two-particle functions g_{12},f_{12}, N_{12} and C_{12} become functions of relative distance only, $F_{12}=F(|\vec{r}_1-\vec{r}_2|)\equiv F(r)$. Equation (19) reduces then to

$$\rho_0\int d^3r\left\{V(r)g(r)+\frac{\hbar^2}{m}\left[\left[\frac{d}{dr}\sqrt{g(r)}\right]^2-\tfrac{1}{4}g'(r)N'(r)-\tfrac{1}{8}N'(r)C'(r)\right]\right\}=\mu\ . \tag{23}$$

This defines an expression for the bulk pressure since we know the chemical potential

$$\mu\equiv\frac{E_B}{N}+\frac{P}{\rho_0} \tag{24}$$

and the energy per particle in a uniform system

$$\frac{E_B}{B}=\tfrac{1}{2}\rho_0\int d^3r\left\{V(r)g(r)+\frac{\hbar^2}{m}\left[\left[\frac{d}{dr}\sqrt{g(r)}\right]^2-\tfrac{1}{4}g'(r)N'(r)\right]\right\} . \tag{25}$$

Therefore

$$\frac{P}{\rho_0}\equiv\mu-\frac{E_B}{N}=\frac{E_B}{N}-\frac{\hbar}{8m}\rho_0\int d^3r\,N'(r)C'(r)\ . \tag{26}$$

As one can see this expression for the pressure agrees with that obtained in Refs. 32 and 3. This becomes more explicit if we write it in terms of the structure function $S(k)$,

$$S(k)=1+\rho_0\int d^3r\,e^{i\vec{k}\cdot\vec{r}}[g(r)-1]\ . \tag{27}$$

The Fourier transform of the nodal sum $N(r)$ and the direct correlation function $C(r)$ are also functions of $S(k)$:

$$N(k)=\frac{[S(k)-1]^2}{S(k)}\ , \tag{28}$$

$$C(k)=\frac{S(k)-1}{S(k)}\ . \tag{29}$$

This leads to the expression (24) in Ref. 3:

$$\frac{P}{\rho_0}=\frac{E_B}{N}-\frac{\hbar^2}{8m\rho_0}\int\frac{d^3k}{(2\pi)^3}k^2\frac{(S-1)^3}{S^2}\ . \tag{30}$$

The second Euler equation (20) reduces in the case of uniform system to

$$-\frac{\hbar^2}{m}\nabla^2\sqrt{g(r)}+\sqrt{g(r)}[V(r)+W_g(r)]=0 \tag{31}$$

with the induced potential used in earlier works[3,4]:

$$W_g(r)\equiv\frac{\hbar^2}{2m}\left[\nabla^2N(r)-\frac{\rho_0}{2}\int d^3r_3C'_{13}C'_{32}\right]=-\frac{\hbar^2}{4m}\int\frac{d^3k}{(2\pi)^3\rho_0}e^{i\vec{k}\cdot\vec{r}}k^2\frac{(S-1)^2(2S+1)}{S^2}\ . \tag{32}$$

Hence the generalized Euler equations have the standard uniform density solution. The translational symmetry is broken by the single-particle potential $U_{\rm ext}$. For the calculation of the surface profile the external field is used to make the pressure outside and inside the fluid the same. Thus the strength of $U_{\rm ext}$ will be proportional to the bulk pressure. Our geometry is such that the z axis is normal to the surface and points out from the fluid.

In this work we have used the potential

$$U_{\rm ext}(z)=\frac{P}{\rho_0}\frac{1}{1+\exp[-B(z-z_0)]} . \tag{33}$$

The results, as we shall show in Sec. V, are of course independent on the location z_0 and only very weakly dependent on the thickness parameter B.

In this geometry the density $\rho(z)$ depends only upon z, and the two-particle functions depend upon z_1,z_2 and the variable $|\vec{\eta}_1-\vec{\eta}_2|$ where $\vec{\eta}=\vec{r}-(\vec{r}\cdot\hat{z})\hat{z}$ is the coordinate in the plane perpendicular to $\hat{z}$.

A simultaneous solution of two nonlinear integro-differential Euler equations together with the Ornstein-Zernike integral equation is currently beyond the capacity of our computer facilities. Since our main interest lies in the density profile we separate the Euler equations and solve Eq. (19) exactly for given g_{12} and N_{12}. The two-particle functions are calculated from Eq. (20) at 30 different constant densities. Thus we get tabulation of functions

$$g_{12}=g(|\vec{r}_1-\vec{r}_2|,\bar{\rho})$$

and (34)

$$N_{12}=N(|\vec{r}_1-\vec{r}_2|,\bar{\rho}) .$$

The tables are then used in Eq. (19). The coupling of these solutions to the density profile emerges through the two choices of the density parameter $\bar{\rho}$ we have used in this work:

$$\bar{\rho}=\begin{cases}\left[\rho(z_1)\rho(z_2)\right]^{1/2}\\ \frac{1}{2}[\rho(z_1)+\rho(z_2)].\end{cases} \tag{35}$$

These local-density approximations have been widely used in earlier calculations.[23,24] The main improvement here is that both g_{12} and N_{12} will be optimized as we shall discuss in the next section.

III. THE TWO-PARTICLE FUNCTIONS g_{12} AND N_{12}

The technique for solving the radial distribution function g_{12} and the nodal sum N_{12} or equivalently the Jastrow factor f_{12} for the uniform ^{4}He fluid is described in Ref. 3. We have followed their procedure by linearizing the Euler equation (31) for $\sqrt{g(r)}$ and iterating the linearized equation. The iteration converges rapidly if a reasonable starting function for $g(r)$ is used. The other functions $N(r)$, $C(r)$, and $f(r)$ can always be obtained from $g(r)$ using Eqs. (9) and (27)–(29). The iteration scheme is repeated for 30 different densities between 0.001 and 0.023 Å^{-3} in order to provide enough points for spline interpolation which is employed when functions g, N, and C are used in the Euler equation for the density.

The optimizing equation (31) leads to difficulties at small densities because it does not have a physical solution below the spinodal density $\rho_{\rm sp}$. The breakdown happens at $\rho_{\rm sp}\sim 0.016$ Å^{-3} when the Lennard-Jones potential

$$V(r)=4\epsilon\left[\left(\frac{\sigma}{r}\right)^{12}-\left(\frac{\sigma}{r}\right)^{6}\right] \tag{36}$$

with de Boer–Michels parameters $\sigma=2.556$ Å and $\epsilon=10.22$ K is used.

The dominant feature of the pair distribution function at small densities is determined by the fact that there is a strong repulsion between ^{4}He atoms. A reasonable model could be a system of billiard balls with a fixed hard-core radius.[29] We prefer, however, that the energy per particle of ^{4}He matter remains negative all the way to zero density. Thus some attraction is needed. A prescription that fulfills that requirement and yet is capable of producing a stable physical solution is to reduce the attractive part of the Lennard-Jones potential linearly at densities below the spinodal density,

$$\bar{V}(r)=\begin{cases}V(r) & \text{when } V\geq 0\\ a(\bar{\rho})V(r) & \text{when } V\leq 0,\end{cases} \tag{37}$$

where

$$a(\bar{\rho})=\begin{cases}1 & \text{when } \rho\geq\rho_{\rm sp}\\ \dfrac{\bar{\rho}}{\rho_{\rm sp}} & \text{when } \bar{\rho}\leq\rho_{\rm sp}.\end{cases} \tag{38}$$

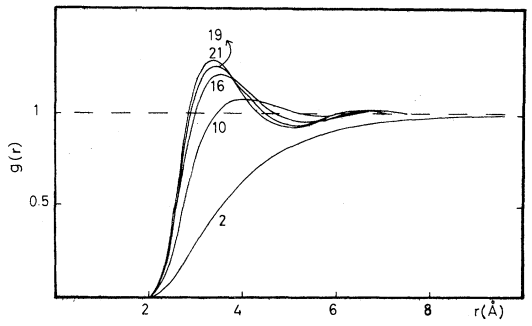

FIG. 1. Radial distribution function $g(r)$ evaluated at different bulk densities (in units 10^{-3} Å^{-3}).

In this way we keep the repulsive core fixed.

The resulting $g(r)$ and $S(k)$ are shown in Figs. 1 and 2. One should obtain $S(0)=0$ from an accurate calculation. The fact that $S(0)\neq 0$ in our work is due to the cutoff in the r-space integration where $r_{\max}=20$ Å. For the present purposes, however, this is completely sufficient and has no further consequences to the results we present. In Fig. 3 we plot the bulk energy per particle, pressure, and chemical potential as a function of density. As required the energy per particle remains negative at all densities of interest.

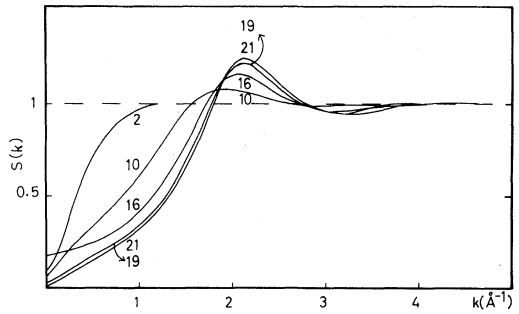

FIG. 2. Structure functions $S(k)$ evaluated at the same bulk densities as $g(r)$.

IV. THE ONE-PARTICLE DENSITY

We return now to the solution of the first Euler equation (19). Inserting the cylindrical symmetry of the planar surface and the local-density approximation for the two-particle functions g_{12}, N_{12}, and C_{12}, we can write the equation for $\sqrt{\rho(z)}$ in the following form:

$$-\frac{\hbar^2}{2m}\frac{d^2}{dz^2}\sqrt{\rho(z)}+\sqrt{\rho(z)}[W_\rho(z)+U_{\text{ext}}(z)]=\mu\sqrt{\rho(z)}\ , \tag{39}$$

where

$$W_\rho(z)=\epsilon(z)+\frac{1}{\rho_0}P(z) \tag{40}$$

with

$$\epsilon(z)=\int_{-\infty}^{\infty}dz'\rho(z')\pi\int_{|z-z'|}^{\infty}r\,dr\left\{V(r)g(r,\bar\rho)+\frac{\hbar^2}{m}\left[\left[\frac{d}{dr}\sqrt{g(r,\bar\rho)}\right]^2-\tfrac{1}{4}g'(r,\bar\rho)N'(r,\bar\rho)\right]\right\} \tag{41}$$

and

$$\frac{1}{\rho_0}P(z)=\epsilon(z)-\frac{\hbar^2}{4m}\pi\int_{-\infty}^{\infty}dz'\rho(z')\int_{|z-z'|}^{\infty}r\,dr\,C'(r,\bar\rho)N'(r,\bar\rho)\ . \tag{42}$$

The structure of Eq. (39) is the same as the one for $\sqrt{g(r)}$ in a sense that it is a nonlinear integrodifferential equation. Thus the same linearization technique can be applied by writing $\sqrt{\rho}\to\sqrt{\rho_n}+\Delta(z)$,

$$-\frac{\hbar^2}{2m}\Delta''(z)+\Delta(z)[U_{\text{ext}}(z)+W_\rho(z)-\mu]+\sqrt{\rho(z)}\int_{-\infty}^{\infty}dz'\sqrt{\rho(z')}\Delta(z')\delta W(|z-z'|,\bar\rho)$$
$$=\frac{\hbar^2}{2m}\frac{d^2}{dz^2}\sqrt{\rho_n(z)}-[U_{\text{ext}}(z)+W_\rho(z)-\mu]\sqrt{\rho_n(z)}\ , \tag{43}$$

where

$$\delta W(|z-z'|,\bar\rho)=4\pi\int_{|z-z'|}^{\infty}r\,dr V(r)g(r,\bar\rho)$$
$$+\frac{\hbar^2}{m}\left[\left[\frac{d}{dr}\sqrt{g(r,\bar\rho)}\right]^2-\tfrac{1}{4}[g'(r,\bar\rho)+C'(r,\bar\rho)]N'(r,\bar\rho)-C(r,\bar\rho)\mathcal{I}(r,\bar\rho)\right]\ . \tag{44}$$

In the last term of the function $\mathcal{I}(r,\bar\rho)$ is a constant density approximation of the integral

$$\mathcal{I}(r,\bar\rho)=\tfrac{1}{4}\int d^3r_3\rho_3\vec\nabla_3C_{13}\cdot\vec\nabla_3C_{32}\approx\frac{1}{8\pi^2\bar\rho r}\int k^3dk\sin(kr)\left[\frac{S(k,\bar\rho)-1}{S(k,\bar\rho)}\right]^2\ . \tag{45}$$

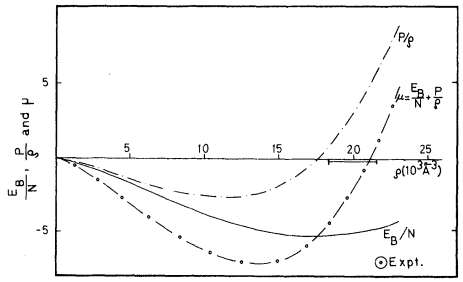

FIG. 3. Energy per particle E_B/N, pressure P, and chemical potential μ as a function of density.

This approximation affects only the rate of convergence in the iteration but has no effect on final results.

The iteration procedure is such that for given $\sqrt{\rho_n(z)}$ we obtain $\Delta(z)$ from Eq. (43). The new function $\sqrt{\rho_{n+1}(z)}=\Delta(z)+\sqrt{\rho_n(z)}$ is inserted into the linearized equation and iteration is continued until $\Delta(z)<10^{-4}\sqrt{\rho_0}$ at all values of z. Starting from a Fermi distribution

$$\rho(z)=\frac{\rho_0}{1+e^{\alpha z}}\ , \tag{46}$$

some 50 iterations are needed. The parameter α may be determined from the asymptotic behavior of Eq. (39) when $z\to\infty$

$$\alpha=\left[\frac{-2m}{\hbar^2}\frac{E_B}{N}\right]^{1/2}. \tag{47}$$

It is interesting to note that we can relate through the Euler equation (39) the definition (12) of the surface energy E_s to a mechanical definition of surface tension γ adopted by Kirkwood and Buff.[30] Multiplying Eq. (39) by $\sqrt{\rho(z)}$ and integrating over z we get an equation

$$\begin{aligned}E_s&=\frac{\hbar^2}{2m}\int dz\left[\frac{d}{dz}\sqrt{\rho(z)}\right]^2\\&\quad+\int dz\rho(z)\left[\epsilon(z)+U_{\rm ext}(z)-\frac{E_B}{N}\right]\\&=\int_{-\infty}^{\infty}dz\frac{\rho(z)}{\rho_0}[P-P(z)]\equiv\gamma\ .\end{aligned} \tag{48}$$

The left-hand side equals to the surface energy E_s and the right-hand side is the Kirkwood-Buff definition for the surface tension γ where $P(z)$ describes the pressure parallel to the surface.

Finally we define the free-surface energy

$$E_s^{\rm free}=\gamma_F=\gamma-\int_{-\infty}^{\infty}dz\,\rho(z)U_{\rm ext}(z) \tag{49}$$

by subtracting the external field. This is the quantity we shall quote in numerical results.

V. RESULTS AND DISCUSSION

The hypernetted-chain theory appears to be a fruitful approximation in the study of the surface properties of Bose fluids. The Euler equations that optimize the density profile and the pair distribution function can be obtained by a straightforward variation of the free energy of the system. Thus they provide an exact starting point for our calculations.

In Sec. III we already briefly discussed the results for the uniform liquid ^{4}He which are summarized in Fig. 3. One finds there that our model saturates at the density $\rho_0=0.0175$ Å^{-3} with the energy $E_B/N=-5.2$ K. This is quite far from the experimental saturation point $\rho_0=0.021\,85$ Å^{-3} and $E_B/N=-7.14$ K. In one of the previous works[23] it was suggested that the strength of the Lennard-Jones potential should be increased by a factor of 1.09. This indeed lowers the saturation energy but leaves the saturation density almost unchanged. That is because the multiplicative factor increases also the repulsive part of the potential. It has also been shown[31] that in the Green's function Monte Carlo calculations the saturation properties of ^{4}He are quite well described even with the potential of Eq. (36). Thus we have chosen to leave the Lennard-Jones potential unchanged and present results in the HNC approximation. In Fig. 3 we have also plotted the chemical potential. It becomes zero at $\rho_0=0.021$ Å^{-3} and is positive at larger densities. This means that the free surface for liquid ^{4}He can exist only with the bulk densities below 0.021 Å^{-3}. In the numerical calculations this shows up in two ways; the convergence of the iteration above the critical density becomes very slow making it difficult to find a consistent solution and the free-surface energy defined by Eq. (49) turns negative. We are hesitant in claiming physical consequences from the breakdown of the solution at large densities or equivalently at high pressures, because other effects like solidification may make the concept of the free surface meaningless.

In Fig. 4 we give the free-surface energy as a function of ρ_0 using three different approximations. The density range where we find solutions is bounded now from two sides. In the high-density limit, discussed above, the free-surface energy becomes negative and in the low-density limit the bulk pressure becomes zero. The saturation point cannot be

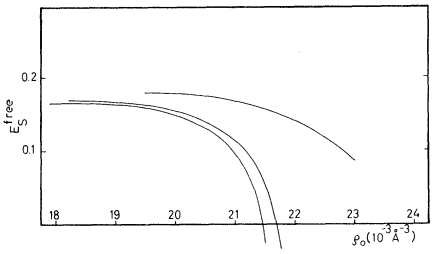

FIG. 4. Free-surface energy E_s^{free} defined in Eqs. (12) and (49) as a function of the bulk density ρ_0. The lowest curve is obtained using the arithmetic mean in the local-density approximation. The geometric mean is used for the curve in the middle and the arithmetic mean together with the small density cutoff for the curve on the top.

quite reached in the numerical work because the external potential U_{ext} is proportional to the pressure and $U_{\text{ext}}>0$ is required in order to provide localization of the surface. The extrapolation of the results to the saturation point, however, is reliable because the shape of the profile and the surface energy remain unaltered for a rather large density range near the saturation point. The lowest curve in Fig. 4 is obtained by using the arithmetic mean $\bar{\rho}=\frac{1}{2}(\rho_1+\rho_2)$. Solutions to Eq. (39) were found in the region $0.0179\ \text{Å}^{-3}\leq\rho_0\leq 0.0215\ \text{Å}^{-3}$. The value of the surface energy extrapolated to the saturation point, $E_s^{\text{free}}=0.167\ \text{K/Å}^2$, is about 30% below the experimental value $0.274\ \text{K/Å}^2$. This discrepancy can be attributed to the lack of binding and to the small saturation density of the uniform liquid in the HNC approximation.[4]

In agreement with Chang and Cohen[23] we find that the use of geometric mean $\bar{\rho}=\sqrt{\rho_1\rho_2}$ makes very little difference near the saturation point as seen from the curve in the middle of Fig. 4. The region where the solution exists with the geometric mean, however, is further shifted from the optimum. Thus we believe that the arithmetic mean is slightly more realistic in describing the coupling between the two-particle functions and the density profile.

The third curve in Fig. 4 is obtained by neglecting the contribution of densities below the spinodal point $\rho_{\text{sp}}=0.016\ \text{Å}^{-3}$ in the evaluation of the two-particle functions. We set there $\bar{\rho}=\frac{1}{2}(\rho_1+\rho_2)\equiv\rho_{\text{sp}}$ if $\bar{\rho}\leq\rho_{\text{sp}}$. The extrapolation of the curve to the saturation point yields $E_s=0.18\ \text{K/Å}^2$, 6% above previous results, but the region where the solution exists is quite far from the optimum. This tells that it is important to take into account the full density dependence of g_{12} and N_{12} when the existence of the solution is studied but it makes little difference near the saturation point. Finally, we point out that if $\bar{\rho}\equiv\rho_0$, the bulk density, or in other words g_{12} and N_{12} are kept independent of $\bar{\rho}$, Eq. (39) does not have a solution at all.

In Fig. 5 we then show a typical surface profile. It is evaluated at $\rho_0=0.0183\ \text{Å}^{-3}$. The Gibb's surface is located to the origin, i.e.,

$$\int_{-\infty}^{\infty}[\rho(z)-\rho_0\Theta(z)]dz=0\ . \tag{50}$$

Here $\Theta(z)$ is a step function. This definition determines the parameter z_0 in U_{ext} yielding $z_0=0.438$. The other parameter B is taken to be 5 Å. Our results are very weakly dependent on it because the variation of B from 3 to 7 gives graphically indistinguishable curves and the surface energy changes only $\sim 5\times 10^{-4}\ \text{K/Å}^2$. The profile is a monotonically decreasing function showing no oscillations. Its thickness is about 6 Å. Thus it is quite diffuse which again is due to the lack of binding in the uniform system. The effective potential $W_\rho(z)-\mu$ appearing in Eq. (39) is also plotted in Fig. 5. It has a minimum at 0.5 Å and only 0.6 K deep. The surface profiles become more diffuse with increasing bulk density as shown in Fig. 6. This happens because the pressure inside the fluid increases and the chemical potential approaches to zero. The fluid then finds increasing difficulty in holding itself together.

As a conclusion we claim that the method developed here provides a reliable basis in describing the physical properties of the free surface of liquid ^{4}He. With enough numerical capacity and patience one could solve the coupled Euler equations in (19) and (20) directly and hence obtain exact results within the HNC approximation. The local-density approximation applied in this work in the evaluation of the optimized g_{12} and N_{12} turned out to be quite accurate. In this approximation it is

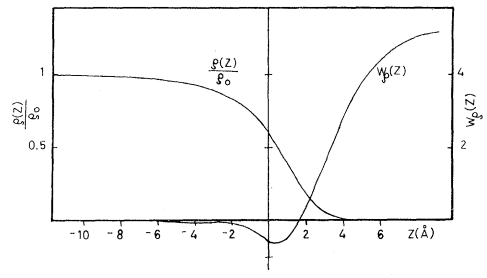

FIG. 5. Density profile $\rho(z)$ and the effective potential $W_\rho(z)-\mu$ from Eq. (40) evaluated at $\rho_0=0.0183\ \text{Å}^{-3}$ with the arithmetic mean.

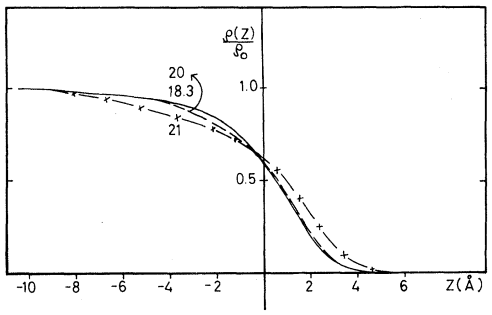

FIG. 6. Density profiles at three different bulk densities using the arithmetic mean. (ρ_0 is in units 10^{-3} Å^{-3}.)

straightforward to solve numerically the Euler equation (39). We believe that our way of constructing the surface energy preserves the variational property of the system. Thus our best result with the arithmetic mean represents an upper limit to the surface energy. In order to obtain a better agreement with the experimental surface-energy measurements one should add elementary diagrams and find a two-particle potential which describes well the saturation properties of the uniform ^{4}He system in the HNC/E approximation.

ACKNOWLEDGMENT

We thank Dr. L. Lantto for many valuable discussions.

[1]C. E. Campbell, *Progress in Liquid Physics* (Wiley, New York, 1978), Chap. 6.
[2]S. Fantoni and S. Rosati, Nuovo Cimento 25A, 593 (1975).
[3]A. D. Jackson, A. Lande, and L. J. Lantto, Nucl. Phys. A 317, 70 (1979).
[4]R. A. Smith, A. Kallio, M. Puoskari, and P. Toropainen, Nucl. Phys. A 328, 186 (1979).
[5]M. Puoskari and A. Kallio, Phys. Scr. 24, 601 (1981).
[6]F. A. Stevens and M. A. Pokrant, Phys. Rev. A 8, 990 (1973).
[7]L. J. Lantto and P. J. Siemens, Nucl. Phys. A 317, 55 (1979).
[8]L. J. Lantto, Phys. Rev. B 22, 1380 (1980).
[9]J. G. Zabolitzky, Phys. Rev. B 22, 2353 (1980).
[10]J. W. Clark, *Progress in Particle and Nuclear Physics* (Pergamon, New York, 1979), Vol. 2.
[11]A. Kallio, P. Pietiläinen, M. Puoskari, and P. Toropainen, Phys. Scr. 22, 91 (1980).
[12]A. Kallio, M. Puoskari, and P. Pietiläinen, in *Recent Progress in Many-Body Theories,* edited by J. G. Zabolitsky (Springer, Berlin, 1981), p. 235.
[13]For a recent review see R. Nieminen and N. W. Ashroft, Phys. Rev. A 24, 560 (1981).
[14]K. R. Atkins and Y. Narahara, Phys. Rev. 138, A437 (1965); J. R. Eckardt, D. O. Edwards, S. Y. Shen, and F. M. Gasparini, Phys. Rev. B 16, 1944 (1977); H. M. Guo, D. O. Edwards, R. E. Sarwinski, and J. T. Tough, Phys. Rev. Lett. 27, 1259 (1971).
[15]D. O. Edwards, P. P. Fatouros, G. G. Ihas, P. Mrozinski, S. Y. Shen, F. M. Gasparini, and C. P. Tam, Phys. Rev. Lett. 34, 1153 (1975).
[16]D. O. Edwards, P. P. Fatouros, G. G. Ihas, P. Mrozinski, S. Y. Shen, and C. P. Tam, *Quantum Statistics and The Many-Body Problem,* edited by S. B. Trickey (Plenum, New York, 1976), p. 195; P. M. Echenique and J. B. Pendry, Phys. Rev. Lett. 37, 561 (1976); J. Phys. C 9, 3183 (1976).
[17]D. O. Edwards and W. F. Saam, *Progress in Low-Temperature Physics,* edited by D. F. Brewer (North-Holland, Amsterdam, 1978), p. 282.
[18]C. A. Croxton, *Statistical Mechanics of the Liquid Surface* (Wiley, New York, 1980), Chap. 6.
[19]R. A. Guyer and M. D. Miller, Phys. Rev. Lett. 42, 1754 (1979); I. B. Mantz, and D. O. Edwards, Phys. Rev. B 20, 4518 (1980).
[20]N. D. Mermin, Phys. Rev. 137, A1441 (1965); P. C. Hohenberg and W. Kohn, *ibid.* 136, B864 (1964).
[21]T. Regge, J. Low Temp. Phys. 9, 123 (1972); T. C. Padmore and M. W. Cole, Phys. Rev. A 9, 802 (1974).
[22]C. Ebner and W. F. Saam, Phys. Rev. B 12, 923 (1975).
[23]C. C. Chang and M. Cohen, Phys. Rev. A 8, 1930 (1973).
[24]Y. M. Shih and C.-W. Woo, Phys. Rev. Lett. 30, 478 (1973).
[25]L. A. Wojcik, Y. M. Shih, and C.-W. Woo, J. Low Temp. Phys. 23, 345 (1975).
[26]K. S. Liu, M. H. Kalos, and G. V. Chester, Phys. Rev. B 12, 1715 (1975).
[27]T. Morita and K. Hiroike, Progr. Theor. Phys. 25, 537 (1961); J. L. Lebowitz and J. K. Percus, J. Math. Phys. 4, 116 (1963).
[28]E. Feenberg, *Theory of Quantum Fluids* (Academic, New York, 1969).

[29]This idea has been used in the case of independent classical fluids. For reference see J. A. Barker and D. Henderson, Rev. Mod. Phys. 48, 587 (1976).
[30]J. G. Kirkwood, and F. P. Buff, J. Chem. Phys. 17, 338 (1949).
[31]M. H. Kalos, M. A. Lee, and P. A. Whitlock, Phys. Rev. B 24, 115 (1981).
[32]K. Hiroike, Prog. Theor. Phys. 27, 342 (1962).